

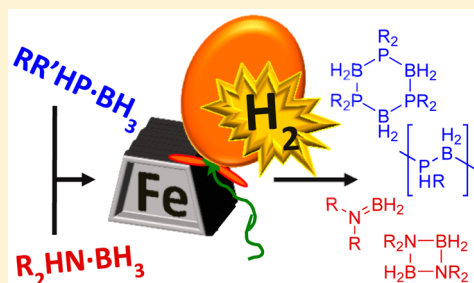
Phosphine- and Amine-Borane Dehydrocoupling Using a Three-Coordinate Iron(II) β -Diketimate Precatalyst

Nathan T. Coles, Mary F. Mahon, and Ruth L. Webster*^{1b}

Department of Chemistry, University of Bath, Claverton Down, Bath BA2 7AY, United Kingdom

S Supporting Information

ABSTRACT: Dehydrocoupling of phosphine- and amine-boranes is reported using an iron(II) β -diketimate complex. Dehydrocoupling of amine-boranes is far more facile than the phosphine counterpart, the former proceeding at room temperature with 1 mol% iron precatalyst. This low loading is sufficient to allow *in situ* kinetic analysis and deuterium labeling studies to be carried out. An iron amido-borane complex has also been isolated, which is believed to be the catalyst resting state. Overall, this has allowed us to postulate a catalytic cycle which proceeds via release of diborane, iron hydride, and iron amido-borane intermediates.



INTRODUCTION

Dehydrocoupling of main group compounds is a powerful tool in sustainable catalysis. For example, the dehydrocoupling of ammonia-borane ($\text{NH}_3\cdot\text{BH}_3$), due to the high yield of H_2 that can be produced relative to the molecular weight of the starting material, means it has the potential to be an efficient and atom-economic method of H_2 storage.^{1–20} Dehydrocoupling of other main group substrates containing diverse functionality (particularly focusing on other amine- and phosphine-boranes) not only provide an alternative to ammonia-borane but can be used to synthesize novel main group compounds or, with judicious selection of substrate, can be used to prepare main group polymers.^{21–36} Alternatively, they proffer excellent opportunities for mechanistic study³² with which new dehydrocoupling catalysis can be developed. In the context of sustainable chemical bond transformations, iron catalysis provides an exceptional opportunity to address many of the challenges of green chemistry, but it is surprising to note that only recently have a handful of iron complexes been reported for amine-borane dehydrocoupling^{37–49} and fewer still for phosphine-borane dehydrocoupling (Figure 1).^{50,51} It has already been shown that simple, three-coordinate iron(II) β -diketimates^{52–55} are highly tunable complexes, undertaking a range of catalytic transformations.^{56–64} With this in mind, we sought to develop dehydrocoupling to tackle a diverse selection of phosphine- and amine-borane substrates while using a well-defined precatalyst to produce a detailed mechanistic investigation of (alkyl)amine-borane dehydrocoupling reactivity.^{44,46}

RESULTS AND DISCUSSION

We initiated our studies by testing three β -diketimate complexes in phosphine-borane dehydrocoupling (1–3, E = P, Scheme 1). The fourth complex (4) has been shown by

Chirik to effect olefin polymerization⁶⁵ and contains the same labile CH_2TMS co-ligand as complexes 1–3.

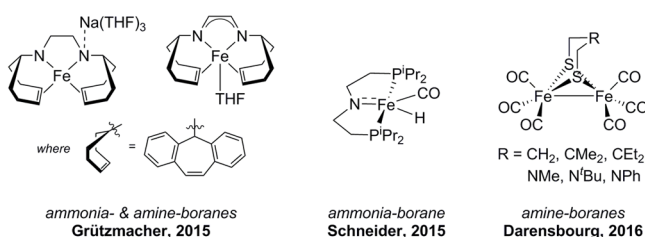
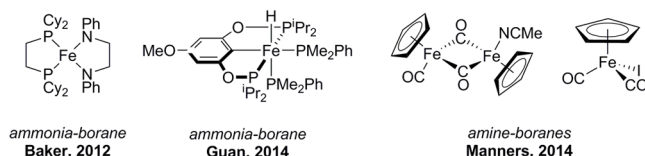
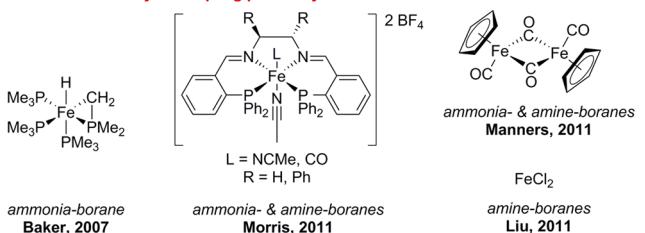
The 2,6-dimethyl complex, 1, gives some dehydrocoupled product 5b after 24 h at 90 °C (Table 1, entry 1), changing to the slightly more bulky 2,6-diisopropyl congener, 2, results in an increase in yield of 5b to 52% under the same reaction conditions (entry 2). A further change in substitution pattern to complex 3 does not increase the yield. Presumably in this instance steric bulk around the iron center is limiting. Precatalyst 4 does not give good levels of dehydrocoupling, and only 36% 5b is obtained (entry 4). This may be unsurprising based on reports from Baker and co-workers on the dehydrocoupling of ammonia-borane where the authors noted that, when using the iron phosphine complex $\text{FeH}(\text{PMe}_2\text{CH}_2)(\text{PMe}_3)_3$, although there was evidence for dehydrocoupling taking place, a black precipitate also formed which was not catalytically active.³⁷ The ¹¹B NMR spectrum recorded also showed the formation of $\text{Me}_3\text{P}\cdot\text{BH}_3$, indicative of catalyst decomposition in the presence of borane-substrate. This is similar to our own observations with precatalyst 4 in the presence of $\text{Ph}_2\text{HP}\cdot\text{BH}_3$ where new phosphine-borane adducts are observed by ³¹P NMR, believed to be ligand-borane adducts.

Using precatalyst 2, we proceeded to optimize the reaction conditions further, finding that 10 mol% 2 and heating to 110 °C gives selective formation of 5a (entries 7 and 8). For comparison, the noncatalyzed reaction requires heating to 170 °C to generate 5a and cyclic tetramer $((\text{Ph}_2\text{P}\text{---}\text{BH}_2)_4)$ in an 8:1 ratio.⁶⁶

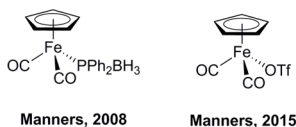
Exploring the substrate scope with phosphine-boranes shows a large dependency on phosphines with phenyl substitution (Table 2, compare entries 1 and 2). Formation of poly-

Received: April 28, 2017

Amine-borane dehydrocoupling pre-catalysts



Phosphine-borane dehydrocoupling pre-catalysts



This work

Phosphine- and amine-borane dehydrocoupling

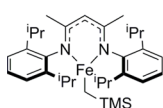
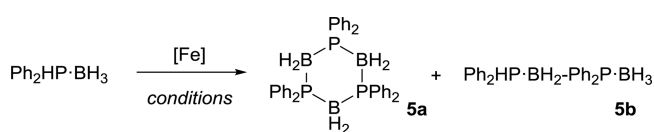


Figure 1. Current examples of discrete iron complexes prepared and implemented in ammine-, amine-, and phosphine-borane dehydrocoupling.

(phosphine-boranes) is successful, and the precipitate of both the high molecular weight (toluene-insoluble) fraction and the lower molecular weight (toluene-soluble) fraction could be separated and analyzed by gel permeation chromatography (GPC) (entry 3). For comparison, Manners achieved $M_n = 59$

Table 1. Optimization of Dehydrocoupling Using $\text{Ph}_2\text{HP}\cdot\text{BH}_3$ as the Standard Substrate



entry	catalyst (loading, mol%)	conditions ^a	spec. yield, % ^b	5a: 5b
1	1 (5)	90 °C, 24 h, C_6D_6	30	0:1
2	2 (5)	90 °C, 24 h, C_6D_6	52	0:1
3	3 (5)	90 °C, 24 h, C_6D_6	43	0:1
4	4 (5)	90 °C, 24 h, C_6D_6	36	0:1
5	2 (10)	90 °C, 72 h, C_6D_6	89	1:1.5
6	2 (5)	110 °C, 72 h, toluene	94	3.3:1
7	2 (10)	110 °C, 72 h, toluene	98	1:0
8	2 (10)	110 °C, 36 h, toluene	95	1:0

^aCommon conditions: $\text{Ph}_2\text{HP}\cdot\text{BH}_3$ (0.25 mmol), solvent (0.5 mL), argon atmosphere. ^bSpectroscopic yield obtained by NMR: ³¹P NMR set with a 50 s relaxation delay and referenced to H_3PO_4 .

kDa and PDI = 1.6 using only 1 mol% $\text{Cp}(\text{CO})_2\text{Fe}(\text{OTf})$ at 100 °C for 24 h, whereas the more coordinating iodide adduct, $\text{Cp}(\text{CO})_2\text{FeI}$, gave $M_n = 18$ kDa after 24 h at 100 °C and required 10 mol% catalyst loading.⁵¹ So although **2** is not competitive with $\text{Cp}(\text{CO})_2\text{Fe}(\text{OTf})$, it is interesting that Manners's change in counterion leads to such a vast change in activity, and this is a potential area for future research in the context of this study. Although a small amount of high molecular weight species is obtained using cyclohexylphosphine-borane polymerizations were run until the starting material was completely consumed. Worthy of note in this respect is Manners and Scheer's elegant metal-free route to poly-(phosphine-boranes) from the corresponding Lewis base stabilized phosphine-borane monomer, which gives access to otherwise challenging to prepare alkyl-substituted products with high M_n and moderate PDI.⁶⁷

Understanding the mechanism of phosphine-borane dehydrocoupling via kinetic analysis is not trivial because of the

Scheme 1. Fe(II) Precatalysts Used To Catalyze the Dehydrocoupling of Phosphine- and Amine-Boranes

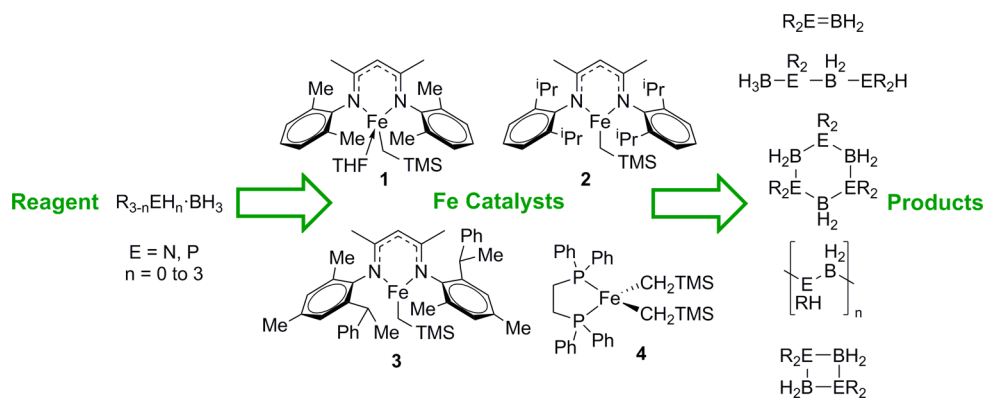


Table 2. Phosphine-Borane Dehydrocoupling Substrate Scope, Catalyzed by 2^a

entry	substrate	product	³¹ P NMR chemical shift, ppm (multiplicity) ^b	spec. yield, % ^c	GPC data
1	Ph ₂ HP·BH ₃		-16.6 (br s)	5a , 95	N/A
2	Cy ₂ HP·BH ₃	Cy ₂ HP·BH ₂ -Cy ₂ P·BH ₃	16.4 (d), -12.2 (s)	5c , <10	N/A
3 ^{d,e}	PhH ₂ P·BH ₃		-43.4 to -59.5 (br s)	5d , 61	M _n = 55.0 kDa PDI = 1.9
4 ^e	CyH ₂ P·BH ₃		-34.0 to -47.0 (br s)	5e , <10	M _n = 54.6 kDa PDI = 1.3

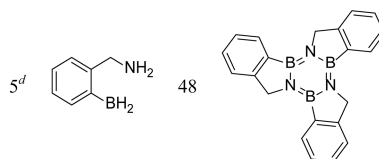
^aConditions: phosphine-borane (0.25 mmol), **2** (14 mg, 10 mol%), toluene (0.5 mL), 110 °C, argon atmosphere. All 72 h except entry 1 (36 h). ^bMultiplicity expressed as br = broad, s = singlet, d = doublet; see [Supporting Information](#) for ¹¹B NMR data and associated spectra. ^cSpectroscopic yield obtained by NMR: ³¹P NMR set with a 50 s relaxation delay referenced to H₃PO₄. ^d6 mol% **2**. Isolated yield of polymer precipitate shown. ^eSpectra for polymerizations are broad: reaction run until complete consumption of starting material. Polymer data measured by GPC eluting with THF. Short oligomeric chains (M_n < 2500 kDa) also obtained; see [Supporting Information](#) for full GPC data.

paramagnetism encountered at fairly high iron loadings. However, preliminary studies are possible. By using the dehydrocoupling of Ph₂HP·BH₃ as the model reaction, addition of a subcatalytic amount of PMe₃ to the reaction mixture does not result in suppression of the formation of **5a**. If the reaction was heterogeneous and iron nanoparticles were present, the addition of a small quantity of phosphine would block the active sites and slow or prevent catalytic turnover.⁶⁸ Over the standard reaction period for this substrate, 99% **5a** forms. The thermal reaction in the absence of catalyst and PMe₃ results in 39% **5b**. We therefore postulate that low levels of noncatalytic dehydrocoupling take place to form the dimeric product, but the presence of catalyst increases the yield of this species. The formation of **5a** under our standard reaction conditions is iron mediated, and this appears to be a homogeneous process. Use of TEMPO as a radical trap or iodo(methyl)cyclopropane as a radical clock does not suppresses the formation of **5a** (99% **5a** after 36 h in the presence of TEMPO at 110 °C with 10 mol% **2**), suggesting that the iron catalyzed aspects are not radical mediated.

In an aim to gain mechanistic insight into heterodehydrocoupling, we decided to investigate amine-boranes ([Table 3](#)). The comparative ease with which these substrates dehydrocouple is exemplified by the vast reduction in reaction temperature, time, and catalyst loading that is needed to facilitate the transformation. In most cases the reaction proceeds using 1 mol% **2** at room temperature. The structures of the products obtained are in line with those reported elsewhere.⁶⁹ Trace amounts of unreacted starting material (and linear dimer **7**, *vide infra*) are observed at the reaction end point for entries 1 and 2. Dehydrocoupling of ammonia-borane is limited by lack of solubility in benzene. Attempts at catalysis in ethereal solvents such as THF or diglyme lead to catalyst decomposition, while solvent mixtures (e.g., diglyme/benzene) or fluorinated solvents (e.g., trifluorotoluene) only give trace amounts of dehydrocoupling. Dehydrocoupling to form

Table 3. Amine-Borane Dehydrocoupling Substrate Scope, Catalyzed by 2^a

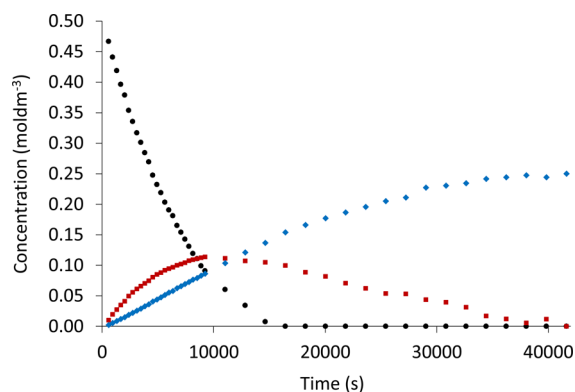
entry	substrate	reaction time, h	product	¹¹ B NMR chemical shift, ppm (multiplicity) ^b	spec. yield, % ^c
1	Me ₂ HN·BH ₃	12	Me ₂ N—BH ₂ H ₂ B—NMe ₂	4.60 (t)	6a , 98
2	MeBnHN·BH ₃	3	MeBnN—BH ₂ H ₂ B—NBnMe	4.3 (m)	6b , 99
3	ⁱ Pr ₂ HN·BH ₃	3	ⁱ Pr N=BH ₂ ⁱ Pr	34.8 (t)	6c , 100
4 ^d	H ₃ N·BH ₃	48	(BH ₂ -NH ₂) _n	—	6d , N.R.



^aConditions: amine-borane (0.25 mmol), **2** (1.4 mg, 1 mol%), C₆D₆ (0.5 mL), room temperature, argon atmosphere. ^bMultiplicity expressed as t = triplet, m = multiplet; see [Supporting Information](#) for coupling constants and associated spectra. ^cSpectroscopic yield obtained by ¹¹B NMR, N.R. = no reaction. ^dIdentical results obtained in C₆D₆, diglyme/C₆D₆ (1:1), and trifluorotoluene. Each reaction performed at room temperature and 40 °C.

borazine **6e** is also hampered by lack of solubility in compatible solvents.

The reaction conditions used to dehydrocouple dimethylamine-borane, to generate **6a**, are perfectly suited to a reaction monitoring study as can be seen from the reaction profile ([Figure 2](#)). Over the course of the reaction the dimer (Me₂HN·

**Figure 2.** Reaction profile showing the consumption of Me₂NH·BH₃ (●) and the formation of **7** (red ■) and **6a** (blue ◆) over time.

BH₂-Me₂N·BH₃, **7**) grows into the reaction mixture and is cyclized to form the product **6a**. Over the course of two half-lives, a first-order relationship in starting material consumption is observed for the standard reaction (0.5 M Me₂HN·BH₃, see [Supporting Information](#), Figure S3), and there is an initial turnover frequency of 68 h⁻¹ (based on consumption of starting material). Manners showed that 55% yield of **6a** is achieved with 1 mol% of the iron dimer [CpFe(CO)₂]₂ after 4 h with photoirradiation, an almost identical result to our own using 1 mol% **2**. A plot showing the initial rate of reaction of Me₂HN·BH₃ at different concentrations gives data consistent with saturation-type kinetics ([Figure 3](#)). By monitoring the

uptake of starting material at different loadings of **2** the reaction is first order in catalyst (Figure 4).

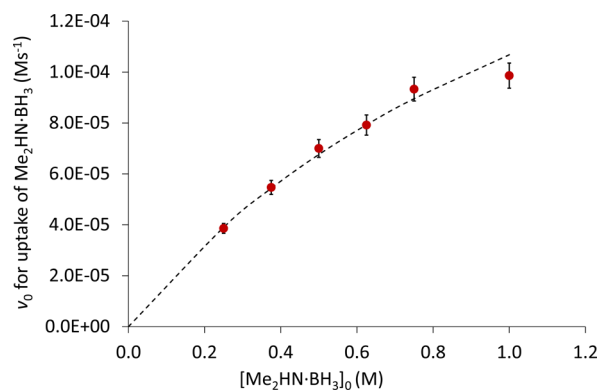


Figure 3. Plot of the initial rate of reaction of $\text{Me}_2\text{NH}\cdot\text{BH}_3$ at various loadings of $\text{Me}_2\text{NH}\cdot\text{BH}_3$, where the line of best fit is a Michaelis–Menten saturation curve.

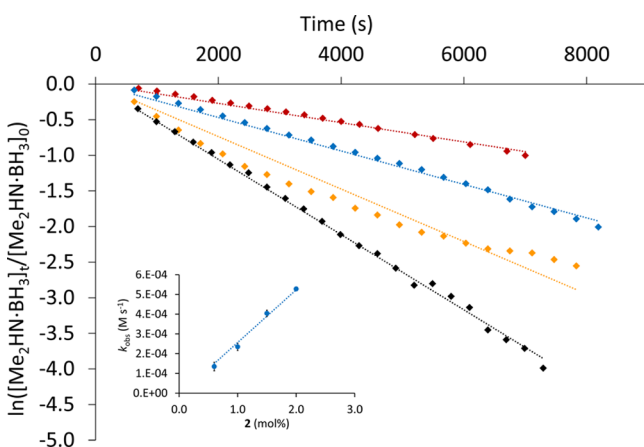


Figure 4. Plot of $\ln([\text{Me}_2\text{NH}\cdot\text{BH}_3]_t/[\text{Me}_2\text{NH}\cdot\text{BH}_3]_0)$ at various catalyst loadings. Reactions were monitored until over 80% $\text{Me}_2\text{NH}\cdot\text{BH}_3$ had been consumed. Standard substrate concentration (0.5 M): black symbols, 2 mol%, $y = -5.28 \times 10^{-4}x$, $R^2 = 99.7$; yellow symbols, 1.5 mol%, $y = -4.04 \times 10^{-4}x$, $R^2 = 92.3$; blue symbols, 1 mol%, $y = -2.35 \times 10^{-4}x$, $R^2 = 99.4$; red symbols, 0.6 mol%, $y = -1.35 \times 10^{-4}x$, $R^2 = 98.8$. Inset: first-order plot for **[2]**.

Deuterium labeling studies using ^{11}B NMR on the uptake of starting material give kinetic isotope effects (KIEs) of 1.7 ± 0.1 for N–H/D, 2.0 ± 0.1 for B–H/D, and 3.0 ± 0.2 when the fully deuterated substrate is employed. KIEs for the formation of product are also moderate: N–H/D 2.5 ± 0.2 , B–H/D 2.1 ± 0.2 , and $\text{Me}_2\text{ND}\cdot\text{BD}_3$ gives a KIE of 3.6 ± 0.3 (see Supporting Information, Figures S12 and S13). The moderate B–D KIE could be consistent with the presence of a nonlinear transition state,⁷⁰ while the KIE for N–D substrate is somewhat lower than expected if N–H cleavage is rate-limiting.⁷¹ However, given the complexity of the catalytic reaction, with the reaction involving the growth of **7**, it is difficult to relate the KIEs obtained to individual steps.⁷²

Synthesis and isolation of potential iron-based intermediates is not trivial; considering the reaction proceeds rapidly at room temperature with only 1 mol% **2**, isolation of the intermediate from a stoichiometric reaction of **2** and $\text{Me}_2\text{NH}\cdot\text{BH}_3$ is challenging. We have been able to synthesize and isolate our postulated reaction intermediates without having to rely on

model compounds (e.g., $\text{R}_3\text{N}\cdot\text{BH}_3$ or $\text{R}_2\text{NH}\cdot\text{BR}'_3$). The iron amido-borane adduct (**8**) can be prepared by reaction of **2** with 1 or 2 equiv of $\text{Me}_2\text{NH}\cdot\text{BH}_3$ at room temperature and is isolated as yellow plates crystallized at -35°C (Figure 5).⁷³

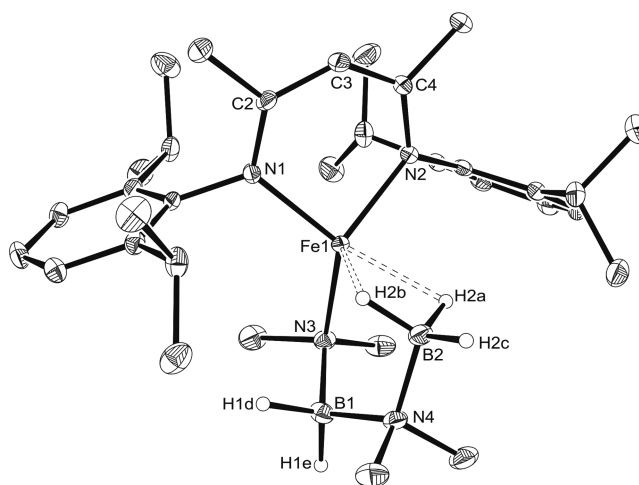


Figure 5. Molecular structure of complex **8**. Ellipsoids are represented at 30%. Hydrogen atoms are omitted for clarity, with the exception of those bound to boron atoms.

When 1 equiv is used, a mixture of **8** and **2** is observed by ^1H NMR. **8** contains short iron–hydride contacts (Fe1–H2A 2.09(3) and Fe1–H2B 1.88(3) Å). However, the X-ray data do not support an assertion that these B–H bonds (B2–H2A 1.18(3) and B2–H2B 1.19(2) Å) are elongated when compared to boron–hydride bonds that are not interacting with the iron center (for example, compare to B2–H2C 1.14(3), B1–H1D 1.15(3), and B1–H1E 1.22(4) Å). The iron hydride dimer (**9**, Figure 6) can also be formed using kinetic control and is synthesized at -78°C . Complex **9** is obtained,⁷⁴ co-crystallized with pentane along with a minor quantity of

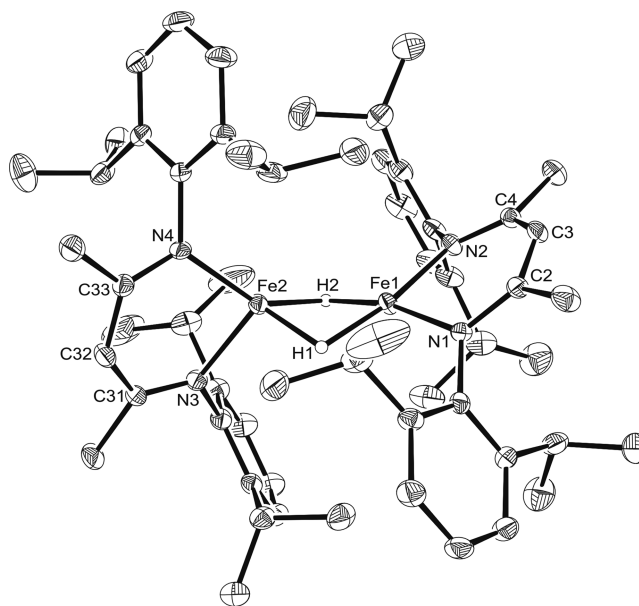
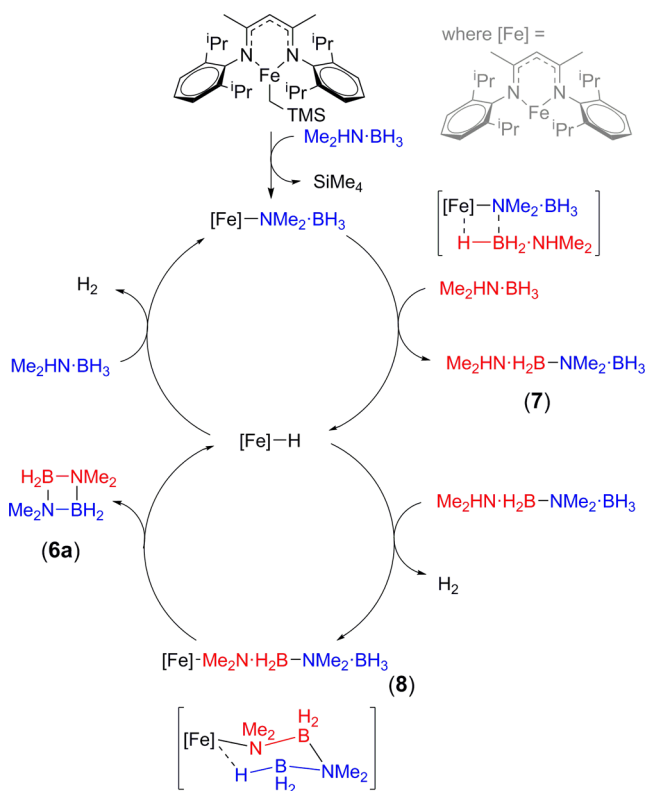


Figure 6. Molecular structure of complex **9**. Ellipsoids are represented at 30%. Hydrogen atoms are omitted for clarity, with the exception of the hydride ligands.

crystals of **8**, as orange rectangular plates and contains iron–hydride bonds that are much shorter than the contacts observed in complex **8** (for **9**, Fe1–H2 1.64(3) and Fe2–H2 1.64(2) Å).⁷⁵ **9** also contains an iron–iron distance of 2.4660(7) Å, which is in agreement with the standard bonding distance anticipated for a bridged Fe–Fe bond.⁷⁶ *In situ* NMR monitoring of a catalytic reaction shows the presence of **8** only. Use of **8** in a catalytic reaction gives a reaction profile and yield of **6a** similar to those obtained using **2** after 12 h at room temperature (see Supporting Information, Figure S9).

Based on our experimental evidence, we tentatively postulate a catalytic cycle which proceeds via a series of σ -bond metathesis steps (Scheme 2). We envisage that the catalyst is

Scheme 2. Proposed Catalytic Cycle for Amine-Borane Dehydrocoupling



activated by dimethylamine-borane, generating an on-cycle iron amido-borane intermediate and releasing $\text{Si}(\text{CH}_3)_4$. As noted, stoichiometric reaction of **2** with 1 equiv of dimethylamine-borane does not give the first on-cycle iron amido-borane intermediate; presumably this species is not long-lived and, during catalysis, undergoes rapid reaction to form **8**. This intermediate therefore quickly reacts with another equivalent of amine-borane, releasing dimeric intermediate **7** and generating an iron hydride. Based on our kinetic data, we propose that the hydride is mononuclear during catalysis, but is crystallized as the more stable dimer, **9**. The hydride has the potential to react with more amine-borane starting material and generate H_2 or, for a productive catalytic process, react with **7** to generate the highly ordered catalyst resting state **8**. Hydride elimination from **8** releases **6a** and generates iron hydride. A small ($\ll 1\%$), constant quantity of sp^2 product $\text{Me}_2\text{N}=\text{BH}_2$ is observed in the reaction mixture. Although we cannot conclusively rule out autocatalytic dimerization of $\text{Me}_2\text{N}=\text{BH}_2$ to form **6a**, we

believe our data is consistent with dehydrogenative cyclization at **8** to form **6a**. This is substantiated by the uniform conversion of **7** into **6a**, as demonstrated by the reaction profile shown in Figure 1, which contrasts with Lloyd-Jones and Weller's leading mechanistic study using an Rh precatalyst that involves $\text{Me}_2\text{N}=\text{BH}_2$ as a key intermediate.⁷⁷ It is also worth noting that when **8** is allowed to decompose to form **6a**, $\text{Me}_2\text{N}=\text{BH}_2$ is not observed at any point. In short, the data are more consistent with mechanistic studies on $\text{Me}_2\text{NH}\cdot\text{BH}_3$ dehydrocoupling which proceed via σ -bond metathesis involving **7**.^{44,69,72,78,79} and similar examples of amine-borane dehydrocoupling which are reported to proceed via σ -bond metathesis involving **7**.^{80,81} **7** has also been prepared via an alternative synthetic procedure (see Supporting Information page 4) and reacted with 5 mol% **2**, giving complete conversion to **6a** within the standard 12 h reaction time, again supporting our proposed mechanism (see Supporting Information, Figures S10 and 11).

Addition of cumene, TEMPO, and chloro(methyl)cyclopropane has no effect on the reaction, which is still complete in 12 h. The reaction mixture is a pale yellow, transparent solution indicating that it is not a heterogeneous reaction, but this is furthered by the addition of a subcatalytic loading of tertiary phosphine (0.2 mol% PMe_3 or PPh_3), which fails to quench the catalysis. Formation of **7** is also consistent with Manners's studies on $\text{CpFe}(\text{CO})_2\text{I}$ -catalyzed dimethylamine-borane dehydrocoupling, which was also determined to be homogeneous (with heterogeneous reactions often favoring $\text{Me}_2\text{N}=\text{BH}_2$ as an intermediate).⁴⁴

CONCLUSIONS

To summarize, we have demonstrated that a three-coordinate Fe(II) complex is catalytically active in the hetero-dehydrocoupling of phosphine- and amine-boranes. Although mechanistic insight into phosphine-borane dehydrocoupling has been hampered by the reaction conditions, we are confident that this reaction is homogeneous and radicals are not involved. The same precatalyst also dehydrocouples amine-boranes via a homogeneous, nonradical mediated process. This is a rare example of heterodehydrocoupling of phosphine- and amine-boranes being undertaken by the same precatalyst and furthermore is one of the few examples of iron catalyzed phosphine-borane dehydrocoupling. We used dimethylamine-borane as a model compound and gained detailed mechanistic insight, postulating a catalytic cycle and isolating an unusual iron chairlike complex, believed to be the catalyst resting state. The reaction mechanism proposed is complementary to those proposed for transition metal catalysts elsewhere in the literature.³²

ASSOCIATED CONTENT

Supporting Information

The Supporting Information is available free of charge on the ACS Publications website at DOI: 10.1021/acs.organomet.7b00326.

Synthetic methods, analysis, and spectroscopic data for all compounds; kinetic plots for all runs (PDF)

Accession Codes

CCDC 1510020 and 1510021 contain the supplementary crystallographic data for this paper. These data can be obtained free of charge via www.ccdc.cam.ac.uk/data_request/cif, or by emailing data_request@ccdc.cam.ac.uk, or by contacting The

Cambridge Crystallographic Data Centre, 12 Union Road, Cambridge CB2 1EZ, UK; fax: +44 1223 336033.

AUTHOR INFORMATION

Corresponding Author

*E-mail r.l.webster@bath.ac.uk.

ORCID

Ruth L. Webster: 0000-0001-9199-7579

Notes

The authors declare no competing financial interest.

ACKNOWLEDGMENTS

The University of Bath is thanked for a DTA studentship (NTC). We gratefully acknowledge Dr. Nicholas P. Taylor for discussions and assistance with kinetic analysis. Dr. George R. Whittell (University of Bristol) is thanked for poly(phosphine-borane) GPC analysis and the group of Dr. G. D. Pantoş for providing a sample of 2-(boranylmethyl)aniline.

REFERENCES

- (1) Stephens, F. H.; Pons, V.; Baker, R. T. *Dalton Trans.* **2007**, 2613–2626.
- (2) Crabtree, R. H. *Energy Environ. Sci.* **2008**, *1*, 134–138.
- (3) Peng, B.; Chen, J. *Energy Environ. Sci.* **2008**, *1*, 479–483.
- (4) Wang, P.; Kang, X.-d. *Dalton Trans.* **2008**, 5400–5413.
- (5) Hamilton, C. W.; Baker, R. T.; Staubitz, A.; Manners, I. *Chem. Soc. Rev.* **2009**, *38*, 279–293.
- (6) Umegaki, T.; Yan, J.-M.; Zhang, X.-B.; Shioyama, H.; Kuriyama, N.; Xu, Q. *Int. J. Hydrogen Energy* **2009**, *34*, 2303–2311.
- (7) Jain, I. P.; Jain, P.; Jain, A. *J. Alloys Compd.* **2010**, *503*, 303–339.
- (8) Jiang, H.-L.; Singh, S. K.; Yan, J.-M.; Zhang, X.-B.; Xu, Q. *ChemSusChem* **2010**, *3*, 541–549.
- (9) Liu, C.; Li, F.; Ma, L.-P.; Cheng, H.-M. *Adv. Mater.* **2010**, *22*, E28–E62.
- (10) Smythe, N. C.; Gordon, J. C. *Eur. J. Inorg. Chem.* **2010**, 2010, 509–521.
- (11) Staubitz, A.; Robertson, A. P. M.; Manners, I. *Chem. Rev.* **2010**, *110*, 4079–4124.
- (12) Jiang, H.-L.; Xu, Q. *Catal. Today* **2011**, *170*, 56–63.
- (13) Sanyal, U.; Demirci, U. B.; Jagirdar, B. R.; Miele, P. *ChemSusChem* **2011**, *4*, 1731–1739.
- (14) Yadav, M.; Xu, Q. *Energy Environ. Sci.* **2012**, *5*, 9698–9725.
- (15) Zhang, J.; Lee, J. W. *Korean J. Chem. Eng.* **2012**, *29*, 421–431.
- (16) Moussa, G.; Moury, R.; Demirci, U. B.; Sener, T.; Miele, P. *Int. J. Energy Res.* **2013**, *37*, 825–842.
- (17) Lin, Y.; Mao, W. L. *Chin. Sci. Bull.* **2014**, *59*, 5235–5240.
- (18) Ley, M. B.; Meggouh, M.; Moury, R.; Peinecke, K.; Felderhoff, M. *Materials* **2015**, *8*, 5891–5921.
- (19) He, T.; Pachfule, P.; Wu, H.; Xu, Q.; Chen, P. *Nat. Rev. Mater.* **2016**, *1*, 16059.
- (20) Ren, J.; Musyoka, N. M.; Langmi, H. W.; Mathe, M.; Liao, S. *Int. J. Hydrogen Energy* **2017**, *42*, 289–311.
- (21) Zybilla, C. E.; Liu, C. Y. *Synlett* **1995**, 1995, 687–699.
- (22) Riedel, R.; Bill, J.; Kienzle, A. *Appl. Organomet. Chem.* **1996**, *10*, 241–256.
- (23) Gauvin, F.; Harrod, J. F.; Woo, H. G., Catalytic dehydrocoupling: A general strategy for the formation of element-element bonds. In *Advances in Organometallic Chemistry*; Stone, F. G. A., West, R., Eds.; Academic Press Limited: London, 1998; Vol. 42, pp 363–405.
- (24) Harrod, J. F. *Coord. Chem. Rev.* **2000**, 206–207, 493–531.
- (25) Brunel, J. M.; Faure, B.; Maffei, M. *Coord. Chem. Rev.* **1998**, *178–180*, 665–698.
- (26) McWilliams, A. R.; Dorn, H.; Manners, I., New Inorganic Polymers Containing Phosphorus. In *New Aspects in Phosphorus Chemistry*; Majoral, J.-P., Ed.; Springer: Berlin/Heidelberg, 2002; Vol. 220, pp 141–167.
- (27) Priegert, A. M.; Rawe, B. W.; Serin, S. C.; Gates, D. P. *Chem. Soc. Rev.* **2016**, *45*, 922–953.
- (28) Clark, T. J.; Lee, K.; Manners, I. *Chem. - Eur. J.* **2006**, *12*, 8634–8648.
- (29) Waterman, R. *Curr. Org. Chem.* **2008**, *12*, 1322–1339.
- (30) Less, R. J.; Melen, R. L.; Wright, D. S. *RSC Adv.* **2012**, *2*, 2191–2199.
- (31) Leitao, E. M.; Jurca, T.; Manners, I. *Nat. Chem.* **2013**, *5*, 817–829.
- (32) Waterman, R. *Chem. Soc. Rev.* **2013**, *42*, 5629–5641.
- (33) Johnson, H. C.; Hooper, T. N.; Weller, A. S., The Catalytic Dehydrocoupling of Amine-Boranes and Phosphine-Boranes. In *Synthesis and Application of Organoboron Compounds*; Fernández, E., Whiting, A., Eds.; Springer: Berlin/Heidelberg, 2015; Vol. 49, pp 153–220.
- (34) Melen, R. L. *Chem. Soc. Rev.* **2016**, *45*, 775–788.
- (35) Rossin, A.; Peruzzini, M. *Chem. Rev.* **2016**, *116*, 8848–8872.
- (36) Stennett, T. E.; Harder, S. *Chem. Soc. Rev.* **2016**, *45*, 1112–1128.
- (37) Keaton, R. J.; Blacquire, J. M.; Baker, R. T. *J. Am. Chem. Soc.* **2007**, *129*, 1844–1845.
- (38) Luo, W.; Campbell, P. G.; Zakharov, L. N.; Liu, S.-Y. *J. Am. Chem. Soc.* **2011**, *133*, 19326–19329.
- (39) Vance, J. R.; Robertson, A. P. M.; Lee, K.; Manners, I. *Chem. - Eur. J.* **2011**, *17*, 4099–4103.
- (40) Baker, R. T.; Gordon, J. C.; Hamilton, C. W.; Henson, N. J.; Lin, P.-H.; Maguire, S.; Murugesu, M.; Scott, B. L.; Smythe, N. C. *J. Am. Chem. Soc.* **2012**, *134*, 5598–5609.
- (41) Duman, S.; Metin, Ö.; Özkaz, S. *J. Nanosci. Nanotechnol.* **2013**, *13*, 4954–4961.
- (42) Sonnenberg, J. F.; Morris, R. H. *ACS Catal.* **2013**, *3*, 1092–1102.
- (43) Bhattacharya, P.; Krause, J. A.; Guan, H. *J. Am. Chem. Soc.* **2014**, *136*, 11153–11161.
- (44) Vance, J. R.; Schäfer, A.; Robertson, A. P. M.; Lee, K.; Turner, J.; Whittell, G. R.; Manners, I. *J. Am. Chem. Soc.* **2014**, *136*, 3048–3064.
- (45) Glüer, A.; Förster, M.; Celinski, V. R.; Schmedt auf der Günne, J.; Holthausen, M. C.; Schneider, S. *ACS Catal.* **2015**, *5*, 7214–7217.
- (46) Lichtenberg, C.; Viciu, L.; Adelhardt, M.; Sutter, J.; Meyer, K.; de Bruin, B.; Grützmacher, H. *Angew. Chem., Int. Ed.* **2015**, *54*, 5766–5771.
- (47) Lichtenberg, C.; Adelhardt, M.; Gianetti, T. L.; Meyer, K.; de Bruin, B.; Grützmacher, H. *ACS Catal.* **2015**, *5*, 6230–6240.
- (48) Lunsford, A. M.; Blank, J. H.; Moncho, S.; Haas, S. C.; Muhammad, S.; Brothers, E. N.; Darensbourg, M. Y.; Bengali, A. A. *Inorg. Chem.* **2016**, *55*, 964–973.
- (49) Zhang, Y.; Zhang, Y.; Qi, Z.-H.; Gao, Y.; Liu, W.; Wang, Y. *Int. J. Hydrogen Energy* **2016**, *41*, 17208–17215.
- (50) Lee, K.; Clark, T. J.; Lough, A. J.; Manners, I. *Dalton Trans.* **2008**, 2732–2740.
- (51) Schäfer, A.; Jurca, T.; Turner, J.; Vance, J. R.; Lee, K.; Du, V. A.; Haddow, M. F.; Whittell, G. R.; Manners, I. *Angew. Chem., Int. Ed.* **2015**, *54*, 4836–4841.
- (52) Holland, P. L. *Acc. Chem. Res.* **2008**, *41*, 905–914.
- (53) Tsai, Y.-C. *Coord. Chem. Rev.* **2012**, *256*, 722–758.
- (54) Annibale, V. T.; Song, D. *RSC Adv.* **2013**, *3*, 11432–11449.
- (55) Chen, C.; Bellows, S. M.; Holland, P. L. *Dalton Trans.* **2015**, *44*, 16654–16670.
- (56) Gibson, V. C.; Marshall, E. L.; Navarro-Llobet, D.; White, A. J. P.; Williams, D. J. *J. Chem. Soc., Dalton Trans.* **2002**, 4321–4322.
- (57) Zhou, M. S.; Huang, S. P.; Weng, L. H.; Sun, W. H.; Liu, D. S. *J. Organomet. Chem.* **2003**, *665*, 237–245.
- (58) Vela, J.; Smith, J. M.; Yu, Y.; Ketterer, N. A.; Flaschenriem, C. J.; Lachicotte, R. J.; Holland, P. L. *J. Am. Chem. Soc.* **2005**, *127*, 7857–7870.
- (59) Ding, K.; Zannat, F.; Morris, J. C.; Brennessel, W. W.; Holland, P. L. *J. Organomet. Chem.* **2009**, *694*, 4204–4208.
- (60) Cowley, R. E.; Golder, M. R.; Eckert, N. A.; Al-Afyouni, M. H.; Holland, P. L. *Organometallics* **2013**, *32*, 5289–5298.

- (61) Bernoud, E.; Oulié, P.; Guillot, R.; Mellah, M.; Hannedouche, J. *Angew. Chem., Int. Ed.* **2014**, *53*, 4930–4934.
- (62) King, A. K.; Buchard, A.; Mahon, M. F.; Webster, R. L. *Chem. - Eur. J.* **2015**, *21*, 15960–15963.
- (63) Espinal-Viguri, M.; Woof, C. R.; Webster, R. L. *Chem. - Eur. J.* **2016**, *22*, 11605–11608.
- (64) Espinal-Viguri, M.; King, A. K.; Lowe, J. P.; Mahon, M. F.; Webster, R. L. *ACS Catal.* **2016**, *6*, 7892–7897.
- (65) Hoyt, J. M.; Shevlin, M.; Margulieux, G. W.; Krska, S. W.; Tudge, M. T.; Chirik, P. J. *Organometallics* **2014**, *33*, 5781–5790.
- (66) Dorn, H.; Singh, R. A.; Massey, J. A.; Nelson, J. M.; Jaska, C. A.; Lough, A. J.; Manners, I. *J. Am. Chem. Soc.* **2000**, *122*, 6669–6678.
- (67) Marquardt, C.; Jurca, T.; Schwan, K.-C.; Stauber, A.; Virovets, A. V.; Whittell, G. R.; Manners, I.; Scheer, M. *Angew. Chem., Int. Ed.* **2015**, *54*, 13782–13786.
- (68) Sonnenberg, J. F.; Morris, R. H. *Catal. Sci. Technol.* **2014**, *4*, 3426–3438.
- (69) Jaska, C. A.; Temple, K.; Lough, A. J.; Manners, I. *J. Am. Chem. Soc.* **2003**, *125*, 9424–9434.
- (70) O'Ferrall, R. A. M. *J. Chem. Soc. B* **1970**, 785–790.
- (71) For amine KIE studies on transition metal catalysis proceeding via σ -bond metathesis, see: Stubbert, B. D.; Marks, T. J. *J. Am. Chem. Soc.* **2007**, *129*, 6149–6167.
- (72) For a detailed kinetic and mechanistic study on amine-borane DHC which also proceeds via intermediate **7**, see: Sloan, M. E.; Staubitz, A.; Clark, T. J.; Russell, C. A.; Lloyd-Jones, G. C.; Manners, I. *J. Am. Chem. Soc.* **2010**, *132*, 3831–3841.
- (73) See [Supporting Information](#) for crystal data for complex **8** (CCDC 1510020).
- (74) Holland has reported this iron complex previously, see ref **58**.
- (75) See [Supporting Information](#) for crystal data for complex **9** (CCDC 1510021).
- (76) Xie, Y.; Schaefer, H. F.; King, R. B. *J. Am. Chem. Soc.* **2000**, *122*, 8746–8761.
- (77) Sewell, L. J.; Lloyd-Jones, G. C.; Weller, A. S. *J. Am. Chem. Soc.* **2012**, *134*, 3598–3610.
- (78) Vogt, M.; de Bruin, B.; Berke, H.; Trincado, M.; Grutzmacher, H. *Chem. Sci.* **2011**, *2*, 723–727.
- (79) Friedrich, A.; Drees, M.; Schneider, S. *Chem. - Eur. J.* **2009**, *15*, 10339–10342.
- (80) Bellham, P.; Anker, M. D.; Hill, M. S.; Kociok-Kohn, G.; Mahon, M. F. *Dalton Trans.* **2016**, *45*, 13969–13978.
- (81) Liptrot, D. J.; Hill, M. S.; Mahon, M. F.; MacDougall, D. J. *Chem. - Eur. J.* **2010**, *16*, 8508–8515.